MILANKOVITCH FORCING OF EQUILIBRIUM GROUND-ICE ON MARS. Oded Aharonson[1,2], Eran Vos[1], Norbert Schörghofer[2] and Francois Forget[3], [1]Weizmann Institute of Science, Rehovot, Israel [2]Planetary Science Institute, Tucson, Arizona / Honolulu Hawaii, [3]Institut Pierre Simon Laplace Université Paris 6, France (Oded.Aharonson@weizmann.ac.il)

Summary Exchangeable ice deposits are present today on Mars in polar caps and as shallow subsurface mid-latitude ground-ice. Geologic evidence indicates these reservoirs waxed and waned in the past in concert with the emplacement and loss of equatorial glaciers. Here we use a climate model [1], to determine the distribution of the mid-latitude ground ice deposits assumed to be in diffusive vapor equilibrium with the atmosphere, at present and under past orbital configurations. The ground-ice and its distribution have profound consequences for various aspects of Mars climate, not only playing a central role in the water cycle, but also determining the seasonal duration of CO_2 stability at the surface, explored in separate work [2]. The model predictions for the extent of the equilibrium ice-table in the past are successful in matching the latitudinal distribution of terrain softening geologic features previously mapped [3–5] and exposures of sub-surface ice in recently formed craters [6].

Introduction Water vapor exchange between the Martian atmosphere and ice in the shallow subsurface governs the present-day distribution of ground-ice ice on Mars. Ice sheets that form on the surface retreat vertically until covered by an ice-free layer of a thickness that allows for vapor equilibrium between the atmosphere and the ice table. Or, if no ice is present initially but the atmosphere is sufficiently humid and the ground porous, ice is sequestered through thermal pumping of vapor [e.g. 7, 8]. Comparisons of models with remote mapping using neutron and gamma-ray emissions and in-situ observations by the Phoenix lander show that ground-ice within the top few decimeters is in approximate diffusive equilibrium with the mean annual atmospheric humidity at present, a state also expected from lab measurements of the diffusive properties of regolith [e.g. 9].

Water ice has also been detected equatorward of the latitude boundary for equilibrium by recent impacts and exposures at scarps [6, 10–12]. Depending on the thickness of the overlying layer and the lithic content of the ice (which produces a sublimation lag), massive pure ice deposits may be an out-of-equilibrium relic of a recent more humid period.

Calculations of the equilibrium ice table for a past climate period [13, 14] require inputs from a model for the vapor content of the atmosphere. The evolution of the subsurface ice volume depends on the atmospheric humidity and, vice versa, the ice content changes the thermal properties significantly, and therefore influences the state of the atmosphere (such as through the amount of seasonal CO_2 frost). Here, we present calculations of the paleoclimate equilibrium ice table using a coupling between a full 3D Global Climate Model for the atmosphere and an equilibrium ice table model. The model results are compared to the geographic and depth-distribution of recent ice deposits.

Methods We use the LMD-GCM [1] to simulate the climate of Mars at various orbital conditions and surface ice distributions. This model has been extensively tested and calibrated with present-day observations, implements the full water cycle and includes treatment of surface ice, atmospheric vapor and ice clouds. The model used to find the depth of the equilibrium ice table relies on the condition that the saturation vapor density at the mean annual temperature (as function of depth) equals the mean annual vapor density in the atmosphere. Once we identify the depth below which subsurface ice is stable, we assign the thermal inertia of all layers below this depth a value of 1,700 J $m^{-2}K^{-1}s^{-1/2}$, representing ice-cemented soil. The GCM is then restarted, and the process is repeated until the ice table variations from year to year are smaller than one resolution layer. Initialization of the subsurface temperatures is performed with a custom algorithm and we ensure convergence is achieved ($\Delta T < 1$ K).

Results Figure 1 shows the predicted equilibrium ice table for present-day conditions, displayed as a geographic map (c) and the zonal average (a). As found in past models [7, 15, 16], ground ice is stable polewards of $\sim 58^\circ$ latitude in both hemispheres. The Figure also shows similar maps, but for past orbital conditions. Specifically, we compare obliquities 15°, 25.1° (as today), 35°, and 45°, with the remaining orbital elements fixed at their present-day value. Several noteworthy results emerge. At low obliquity of 15°, the distribution of ice retreats polewards, with a boundary reaching 70°latitude. Conversely, at high obliquity, the distribution of stable ground ice extends equatorwards, with regions of stability appearing even at equatorial latitudes, in the Western Tharsis and Arabia Terra regions. The stability in this region results from a combination of favorable thermal properties and geographic variations in atmospheric humidity, and thus a full 3D GCM is required to capture the effect. At obliquity 45°, near the highest value attained in last few Myr, the regions of stability grow in extent, covering up to a third of the low latitudes. The significance of the result that extensive re-

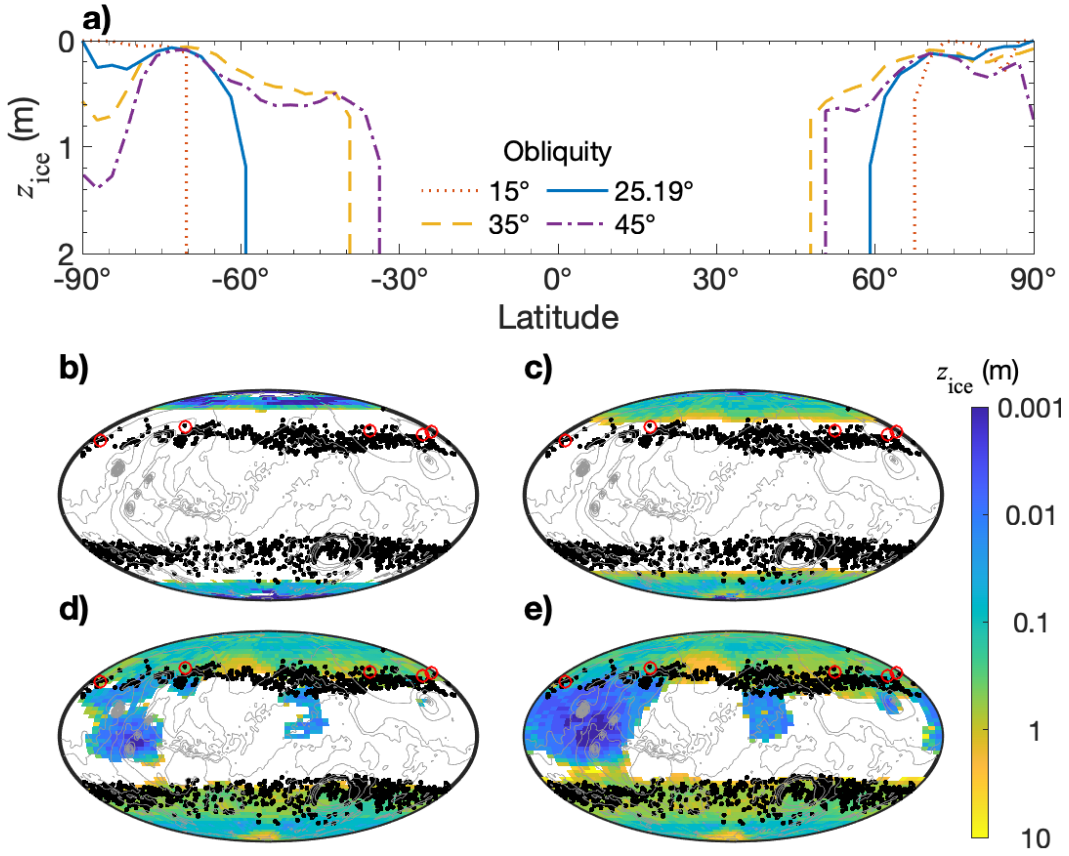

Figure 1: Equilibrium ice-table depth for various obliquities experienced in the past ∼10 Myr. Panels b–e correspond to obliquities of 15°, 25.1°, 35°, and 45°. Black points indicate locations where dissected mantle terrain has been previously mapped [4, 5], and red circles where recent crater events expose subsurface ice deposits [6].

gions of ground-ice stability are present at low latitudes is twofold. It not only suggests the possible diffusive emplacement of ice in the regolith pore space, but also, promotes the stability of ice emplaced by other mechanisms.

In Figure 1 (b-e) we also plot locations where dissected mantle terrain has been mapped [4, 5], and interpreted to indicate atmospheric deposition and subsequent dissection of ice. Latitude-dependent terrain softening features with viscous flow morphology have also been proposed to indicate regions rich in ground ice [3]. The two geomorphic classes share some similar characteristics, appearing over similar latitude bands, mantling pre-existing topography, and showing some evidence of internal layering. A compilation of recent craters found to expose subsurface ice [6] is also shown in the figure. The latitudinal extent of the dissected mantle terrain (and of the smaller number of recently exposed ice deposits) shows remarkable agreement with the maximum extent of the region of ground-ice stability predicted by our model at past obliquities.

References: **[1]** Forget, F. *et al. J. Geophys. Res. Planets* **104,** 24155–24175 (1999). **[2]** David, E., Aharonson, O., Vos, E. & Forget, F. *Lunar & Planet. Sci. Conf.* **1929** (2022). **[3]** Squyres, S. W. & Carr, M. H. *Science* **231,** 249–252 (1986). **[4]** Mustard, J. F., Cooper, C. D. & Rifkin, M. K. *Nature* **412,** 411–414 (2001). **[5]** Milliken, R. E., Mustard, J. F. & Goldsby, D. L. *J. Geophys. Res. Planets* **108** (2003). **[6]** Dundas, C. M., Mellon, M. T., Conway, S. J., *et al. J. Geophys. Res.* **126** (2021). **[7]** Mellon, M. T. & Jakosky, B. M. *J. Geophys. Res.* **98,** 3345–3364 (1993). **[8]** Schorghofer, N. & Aharonson, O. *J. Geophys. Res.* **110,** E05003 (2005). **[9]** Hudson, T. L. *et al. J. Geophys. Res.* **112,** E05016 (2007). **[10]** Byrne, S. *et al. Science* **325,** 1674–1676 (2009). **[11]** Dundas, C. M. *et al. J. Geophys. Res.* **119,** 109–127 (2014). **[12]** Dundas, C. M., Bramson, A. M., Ojha, L., *et al. Science* **359,** 199–201 (2018). **[13]** Mellon, M. T. & Jakosky, B. M. *J. Geophys. Res.* **100,** 11, 781–11, 799 (1995). **[14]** Schorghofer, N. & Forget, F. *Icarus* **220,** 1112–1120 (2012). **[15]** Schorghofer, N. & Aharonson, O. *J. Geophys. Res.* **110** (2005). **[16]** Aharonson, O. & Schorghofer, N. *J. Geophys. Res.* **111** (2006).